RSC Advances

ROYAL SOCIETY OF CHEMISTRY

www.rsc.org/advances

Journal Name

ARTICLE

Boronic acid functionalized magnetic nanoparticles synthesized by atom transfer radical polymerization and their application for selective enrichment of glycoproteins

Received 00th January 20xx,
Accepted 00th January 20xx

DOI: 10.1039/x0xx00000x

www.rsc.org/

Jiewen Wang,[a] Xiwen He,[a] Langxing Chen[a,b,*] and Yukui Zhang[a, c]

Biomedical sciences, especially biomarker research, strongly require efficient glycoproteins enrichment platform. In this work, a facile novel approach is developed for the preparation of boronic acid functionalized Fe_3O_4 magnetic nanoparticles (MNPs) *via* surface-initiated atom transfer radical polymerization (ATRP). Firstly, Fe_3O_4 MNPs were synthesized through a solvothermal method and then the ATRP-initiator was immobilized on the surface of Fe_3O_4 MNPs. Finally, the poly(acrylamidophenylboronic acid) (AAPBA) functionalized Fe_3O_4 MNPs (Fe_3O_4@PAAPBA) were obtained by ATRP technique using affinity monomer 3-acrylamidophenylboronic acid. The morphology, structure and composition of the resulting Fe_3O_4@PAAPBA MNPs were characterized by transmission electron microscopy (TEM), X-ray powder diffraction (XRD), Fourier transform infrared (FTIR) spectroscopy, thermogravimetric analysis (TGA), vibrating sample magnetometer (VSM) and X-ray photoelectron spectrometry (XPS). Four proteins, including ovalbumin (OVA), transferrin (Trf), lysozyme (Lyz), horse heart cytochrome c (Cyt C) are chosen as target proteins in the adsorption performance. The binding capacity towards 1.0 mg mL^{-1} glycoproteins OVA and Trf is 798.1 and 278.1 mg g^{-1} respectively, in contrast, the adsorption of nonglycoproteins is 53.7 mg g^{-1} for Lyz, 30.8 mg g^{-1} for Cyt C. Furthermore, the adsorption-desorption cycle was repeated five times, the Fe_3O_4@PAAPBA MNPs still keep the good binding capacity. The feasibility of glycoproteins enrichment from real egg white samples by Fe_3O_4@PAAPBA was demonstrated. This work could provide a promising method of surface modification for the design of more efficient adsorbents for the isolation and enrichment of proteins from complex bio-samples.

1. Introduction

Protein glycosylation is one of the most complex and ubiquitous posttranslational modifications and plays a significant role in cell attachment-recognition, cell division, immune response, folding of certain proteins, transportation, nerve conduction, regulations of growth and differentiation, and other areas.[1-3] In addition, altered and aberrant glycosylated proteins have been correlated with many human diseases.[4,5] However, the inherent low abundance of glycoproteins in complex biological samples and low ionization efficiency of glycopeptides in mass spectrometry analysis caused by the co-existence abundant non-glycosylated peptides can severely interfere the detection of glycoproteins.[6,7] Therefore, efficient separation and enrichment of glycoproteins from the complex biological samples is indispensable to in-depth research of glycoprotomic analysis.

To date, several strategies based on lectins, hydrazide chemistry, boronate affinity and hydrophilic interaction chromatography[8-15] have been developed for specific recognition or separation of glycoproteins. Among these methods, the lectin affinity enrichment relies on the specific binding between a lectin and a specific glycan, but this interaction has limitations for the biased collection of glycoproteins.[8] The hydrazide chemistry is also widely used, but it is only used for N-linked glycoproteins and the oxidation process is very complicated.[12] Hydrophilic interaction which based on the physical interactions between glycans and the hydrophilic components, has many advantages such as unbiased enrichment towards different glycopeptides, good reproducibility and MS compatibility for the separation of polar compounds, however, it is limited by the insufficient selectivity and recovery.[15] Boronate affinity-based methods has been well developed and gained great interest in recent years due to it has the low-bias, convenience and reversibility.[16-17] Boronic acid can covalently react with cis-diols to form five- or six-membered cyclic esters in a alkaline aqueous

[a] *Research Center for Analytical Sciences,College of Chemistry, Tianjin Key Laboratory of Biosensing and Molecular Recognition, State Key Laboratory of Medicinal Chemical Biology, Nankai University, Tianjin 300071, China*
[b] *Collaborative Innovation Center of Chemical Science and Engineering, Nankai University, Tianjin 300071, China. Email: lxchen@nankai.edu.cn*
[c] *Dalian Institute of Chemical Physics, Chinese Academy of Sciences, Dalian 116023, P. R. China.*

solution and the reversible release can be manipulated by switching to acidic conditions. In recent years, boronic acid ligands-functiontionalized materials such as macroporous monoliths,[18-20] mesoporous silica beads,[21] nanofibers,[22] and magnetic nanoparticles[23-28] have been reported for selective separation and enrichment of glycoproteins and glycopeptides. Among these materials, magnetic nanoparticles (MNPs) recently has become very popularly used in conjunction with biological materials, because the magnetic feature of the solid-phase MNPs can enable them to achieve a rapid and easy separation from the reaction medium in a magnetic field. In order to increase the loading amount of the biomolecules immobilized on magnetic particles and improve the stability of immobilized biomolecules, the procedure of the surface functionalization on the MNPs become the key to the magnetic separation systems.

The various surface modified methods have been used to synthesize boronic acid ligands-functiontionalized MNPs, such as nucleophilic reaction and the ''click-chemistry'' method.[24-27] However, these methods are still challenged by their inherent shortcomings such as the low efficiency of the nucleophilic reaction or the multistep reactions and time-consuming nature of click chemistry. On the other hand, owing to the advantages of various functional groups, facile synthetic process and good biocompatibility, surface-grafted polymers have attracted more and more attention, and become an efficient measure of surface modification.[28] Nevertheless, the intrinsically uncontrollable polymerization rate of the traditional polymerization methods would lead to heterogeneity and low amount of the functional monomers grafted on the particle surface. In recent years, atom transfer radical polymerization (ATRP),[29-34] a type of controlled/living free radical polymerization has become a very popular route to produce many well-defined functional (co)polymers with predefined architectures. Since ATRP could apply a wide range of functional monomers, need less stringent experimental conditions,[31] the graft density via ATRP on the substrate is controlled by the density of the initiator and the chain length by the ratio of monomer to initiator. Besides, surface-initiated atom transfer radical polymerization (SI-ATRP) could avoid the solution-phase polymerization, which endows a high grafting rate on various types of substrate. Therefore, SI-ATRP is expected to play a highly significant role in the preparation of functional materials in separation science field.

In this work, we grafted a homopolymer of boronate functional monomer 3-acrylamidophenylboronic acid (AAPBA) on the surface of Fe_3O_4 MNPs using SI-ATRP. The as-prepared magnetic Fe_3O_4@poly(3-acrylamidophenylboronic acid) (Fe_3O_4@PAAPBA) are expected to have plentiful boronic acid functional groups and high magnetic susceptibility. The Fe_3O_4@PAAPBA MNPs were characterized by transmission electron microscopy (TEM), X-ray powder diffraction (XRD), Fourier transform infrared (FTIR) spectroscopy, thermogravimetric analysis (TGA), vibrating sample magnetometer (VSM) and X-ray photoelectron spectrometry (XPS). The Fe_3O_4@PAAPBA MNPs were applied to enrich several types of glycoproteins and nonglycoproteins, the results show that they have a high binding capacity and an excellent specificity towards glycoproteins. Furthermore, the Fe_3O_4@pAAPBA MNPs were successfully applied in efficient enrichment of target glycoproteins from the egg white real samples.

2 Experimental

2.1 Materials

The proteins ovalbumin (OVA), transferrin (Trf), lysozyme (Lyz), bovine serum albumin (BSA), and cytochrome c (Cyt C) from bovine heart were purchased from Sigma-Aldrich (St. Louis, MO, USA). 3-Aminophenyl-boronic acid monohydrate (APBA·H_2O) was purchased from Beijing East & West Analytical Instruments Ltd (Beijing, China). 2-Bromoisobutyryl-bromide was provided by TCI Shanghai development Co. Ltd. (Shanghai, China). 3-Aminopropyltriethoxysilane (APTES) and 4-dimethylaminopyridine (DMAP) were purchased from J&K Scientific Ltd. (Beijing, China). 1,1',4,7,7'-Pentamethyldiethylenetriamine (PMDETA) was purchased from Aladdin Reagent (Shanghai, China). $FeCl_3·6H_2O$, NaOH, CuBr, anhydrous ammonium acetate (NH_4Ac), disodium phosphate (Na_2HPO_4), sodium citrate, ethanol, ethylene glycol (EG), acetonitrile (ACN), hydrochloric acid, dichloromethane (CH_2Cl_2) and trimethylamine (TEA) were purchased from Tianjin Chemical Reagent Company (Tianjin, China). Deionized water was prepared with a Milli-Q water purification system (Millipore, Milford, MA).

2.2 Preparation of Fe_3O_4 MNPs

Fe_3O_4 MNPs stabilized by citrate groups were prepared according to a modified solvothermal method.[35] Typically, the $FeCl_3·6H_2O$ (0.675 g), NH_4Ac (1.927 g) and sodium citrate (0.200 g) were ultrasonic dissolved in EG (35 ml). Then the homogeneous orange solution was transferred to a Teflon-lined stainless steel autoclave, after reacting at 200℃ for 12h and cooling to room temperature, the resulting Fe_3O_4 MNPs were washed with water and ethanol each for five times, then dried at 50℃ overnight. The resulting Fe_3O_4 MNPs were about 300nm in diameter.

2.3 Preparation of Fe_3O_4@ Initiator MNPs

The Fe_3O_4 MNPs were firstly modified with APTES to introduce amine groups on the surface. This process was achieved by the reaction between APTES and the hydroxyl groups on the surface of the Fe_3O_4 MNPs.[36] Typically, Fe_3O_4 MNPs (600 mg) were dispersed in ethanol (60 ml) by sonication for 20min, then ammonium hydroxide (6.0 ml) was added and sonicated to homogenize for 10 min. The next, under continuous mechanical stirring, 4.0 ml of APTES was added drop by drop to the reaction mixture. After reacting under vigorous mechanical stirring for 8 h at 50℃, the resulting Fe_3O_4@NH_2 MNPs were washed with ethanol to remove unreacted APTES and washed with water until the supernatant was at neutral pH.

The details of the preparation of the Fe_3O_4@Initiator MNPs are as the following.[34] Fe_3O_4 MNPs (300 mg) were dispersed in dichloromethane (26 mL) by sonication for 30min, then, trimethylamine (0.5 mL), DMAP (1.5 mg), 2-bromoisobutyrylbromide (0.4 mL) were added. The mixture was

kept first at 0℃ for 2 hours and then at room temperature for 12 hours. The obtained product was washed with dichloromethane for several times and dried at 40℃ overnight for further use.

2.4 Preparation of the Fe_3O_4@PAAPBA MNPs via SI-ATRP

The boronate-coated MNPs (Fe_3O_4@PAAPBA) were synthesized via an SI-ATRP procedure. First, Fe_3O_4@Initiator MNPs (50 mg) and AAPBA (250 mg) were sonicated to disperse in ACN (10 ml), after performing the freeze–pump–thaw procedure three times to thoroughly remove oxygen, PMDETA (17 μL) and CuBr (8 mg) were quickly added. After mechanically stirred for a while, the freeze – pump – thaw procedure was performed three times again, and the system was proceeded at 70℃ with mechanical stirring for 24 h. The obtained product was washed with ACN and water for several times to remove all unreacted substances.

2.5 Protein adsorption and separation

The adsorption of glycoproteins and nonglycoproteins was carried out by adding the Fe_3O_4@PAAPBA MNPs (2 mg) to a solution (2 ml) of protein samples with different concentrations in 20 mM phosphate buffer solution (PBS) (pH 9.0) containing 0.5 M NaCl, and shaking at room temperature overnight. Then the MNPs were magnetically separated from the solution and the concentration of the supernatant was measured. The adsorption capacity (Q) is calculated using the equation below:

$$Q = (C_0 - C_t)Vm^{-1} \times 10^3 (mg \cdot g^{-1})$$

Here C_0 （mg mL^{-1}） is the initial concentration of protein solution. C_t（mg mL^{-1}） is the equilibrium concentration of the protein; V (mL) is the volume of the protein solution; m (mg) is the mass of the added Fe_3O_4@PAAPBA MNPs. The protein concentration was measured by UV-vis analysis (OVA, Cyt C and Lyz) or by HPLC analysis (Trf).

To estimate the reusability of the Fe_3O_4@PAAPBA MNPs, after the Fe_3O_4@PAAPBA MNPs were incubated with the protein solution, then were separated under the magnet. The adsorbed MNPs were washed twice with 20 mM PBS containing 0.5 M NaCl (pH 9.0) to remove unspecific adsorbed proteins, and then 2mL acidic eluted solution was added to release the glycoproteins. The adsorption-desorption cycle was repeated five times.

2.6 Enrichment of glycoproteins from real egg white samples

The selective adsorption experiment of glycoproteins in real egg white samples was carried out in the following. 2mg Fe_3O_4@PAAPBA MNPs were added into the 200-fold (0.5mL egg white diluted to 100 mL) and 400-fold (0.25mL egg white diluted to 100 mL) dilution of egg white samples in 20 mM PBS solution (pH 9.0) containing 0.5 M NaCl. After shaking overnight, the separated Fe_3O_4@PAAPBA MNPs were washed with 20 mM PBS (pH 9.0) twice and acidic eluted solution was added to elute the adsorbed glycoproteins. Finally, the proteins in the adsorbed and eluted supernatant were analyzed by sodium dodecyl sulfate-polyacrylamide gel electrophoresis (SDS-PAGE).

2.7 Instrumentation

The morphology and structure were examined using a Philips Tecnai G2 T2 S-TWIN transmission electron microscope (TEM) and a Shimadzu SS-550 scanning electron microscope (SEM). Fourier transform IR (FTIR) spectra were determined by using an Nicolet AVATAR-360 FT-IR spectrometer. After vacuum drying, the MNPs samples were thoroughly mixed with KBr (weight ratio of sample/KBr was about 1%) in a mortar, and then pressed into a fine powder. Then the FT-IR spectrum was recorded. The X-ray photoelectron spectra were obtained on a Shimadzu Kratos AXIS Ultra DLD X-ray photoelectron spectrometer (XPS) with Mg Kα anode (15 kV, 400 W) at a take off angle of 45°. The source X-rays were not filtered, and the instrument was calibrated against the C1s band at 285 eV. The identification of the crystalline phase of nanoparticles was performed on a Rigaku D/max/2500v/pc (Japan) X-ray diffractometer (XRD) with a Cu Kα source. The 2θ angles probed were from 3° to 80° at a rate of 4° min^{-1}. The magnetic properties were analyzed with a LDJ 9600^{-1} vibrating sample magnetometer (VSM). Thermogravimetric analysis (TGA) was performed with a NETZSCH TG209 instrument in a nitrogen atmosphere at a heating rate of 10℃ min^{-1} from room temperature to 800℃. Electrophoretic analysis of proteins was performed using regular SDS-PAGE with 15% running and 6% stacking gels. Proteins were stained with Coomassie Brilliant Blue R-250.

3 Results and discussion

3.1 Preparation and characterization of Fe_3O_4@PAAPBA MNPs

In this work, the procedure for the preparation of the Fe_3O_4@PAAPBA MNPs is shown in Figure 1. Firstly, the Fe_3O_4 MNPs stabilized with citrate groups were synthesized by a modified solvothermal method. The TEM image showed that the Fe_3O_4 MNPs

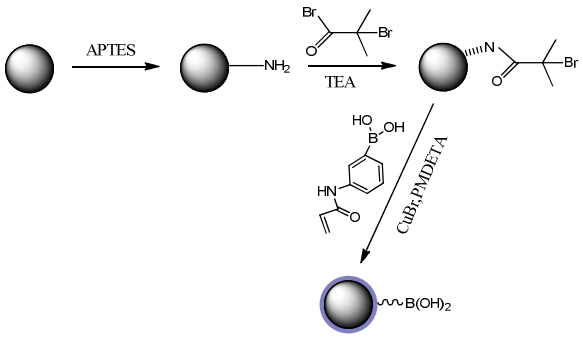

Figure 1 Outline of the fixation of an ATRP initiator onto Fe_3O_4 MNPs and the grafting of AAPBA from Fe_3O_4 MNPs via SI-ATRP.

have an average diameter of about 300 nm. The -NH_2-coated Fe_3O_4 MNPs (Fe_3O_4@NH_2) as a precursor of grafting initiator were prepared by sol–gel reaction with an organosilicon coupling agent APTES. The next, the amino groups of APTES could be easily reacted with 2-bromoisobutyrylbromide to introduce the initiator and the product Fe_3O_4@Initiator MNPs was obtained. Finally, the

affinity monomer 3-acrylamidophenylboronic acid (AAPBA) was successfully grafted on the surface via SI-ATRP.

TEM and SEM images of the synthesized Fe_3O_4, Fe_3O_4@Initiator, and Fe_3O_4@PAAPBA MNPs are displayed in Figure 2. It can be seen that the Fe_3O_4 MNPs were spherical particles with a mean diameter of about 300 nm (Figure 2a and 2d). Because the initiator is grafted via a chemical bonding reaction, after modifying the initiator, it is hard to distinguish the change in diameter and morphology (Figure 2b and 2e). After coating of PAAPBA thin layer, the size of Fe_3O_4@PAAPBA was apparently increased, and the polymer layer is clearly visible (Figure 2c and 2f). To further characterize the size distribution of these MNPs, the particle hydrodynamic size analyzer was displayed in Figure 2g and 2h. The hydrodynamic diameter of the Fe_3O_4 and Fe_3O_4@PAAPBA MNPs was 256±20 and 315±35 nm, respectively. The results of dynamic laser scattering (DLS) for Fe_3O_4 and Fe_3O_4@PAAPBA are close to those measured by TEM.

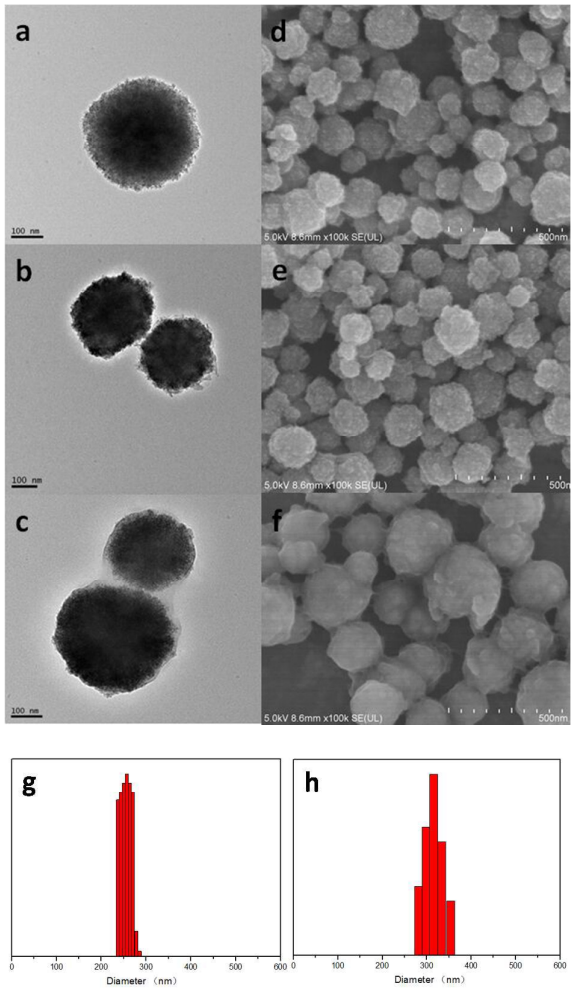

Figure 2 TEM and SEM images of Fe_3O_4(a), (d); Fe_3O_4@Initiator (b), (e) and Fe_3O_4@PAAPBA (c), (f) MNPs, respectively. The particles size distribution of Fe_3O_4(g) and Fe_3O_4@PAAPBA (h) MNPs.

The crystalline structures of the synthesized Fe_3O_4, Fe_3O_4@Initiator, and Fe_3O_4@PAAPBA MNPs were determined by powder X-ray diffraction (XRD). As shown in Figure 3, in the 2θ range of 20–80°, six characteristic peaks (2θ = 30.070, 35.352, 43.012, 53.463, 57.068, 62.689) were observed for the three samples. The peaks at the corresponding 2θ values were indexed to (220), (311), (400), (422), (511), and (440) respectively, which can be matched to the face center-cubic phase of Fe_3O_4 (JCPDS Card No. 19-629). The XRD patterns show that the crystal structure of the magnetic component hasn't changed during the whole modification

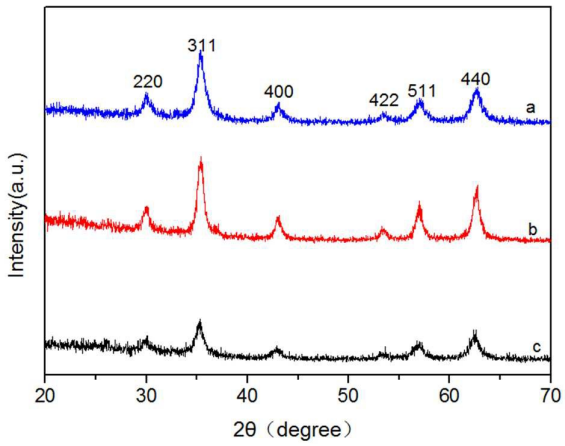

Figure 3 XRD patterns of Fe_3O_4 (a), Fe_3O_4@Initiator (b), and Fe_3O_4@PAAPBA MNPs (c).

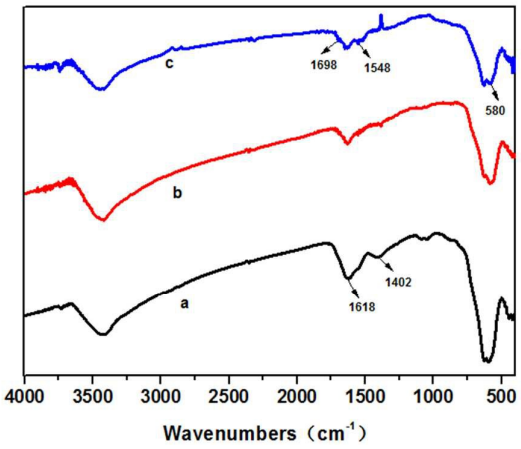

Figure 4 FT-IR spectra of Fe_3O_4 (a), Fe_3O_4@Initiator (b), and Fe_3O_4@pAAPBA MNPs (c).

process.

The FT-IR spectra of Fe_3O_4, Fe_3O_4@Initiator, and Fe_3O_4@PAAPBA MNPs are compared in Figure 4. The bands at about 1618 and 1402 cm^{-1} (Fig. 4a) were attributed to carboxyl groups from the stabilizer citrate and the band at 580 cm^{-1} was associated with the Fe–O bond. The FT-IR spectrum of Fe_3O_4@PAAPBA in Figure 4c shows that the absorption peaks at

1548 and 1698 cm^{-1} could be associated with the bending vibration of N-H and the stretching vibration of C=O bond in amido groups existed in monomer AAPBA. The FT-IR results further confirmed that PAAPBA coating was successfully formed on the Fe_3O_4@Initiator by SI-ATRP.

Vibrating sample magnetometry (VSM) was employed to study the magnetic properties of the synthesized MNPs. The magnetic hysteresis curves show that all MNPs have no obvious remanence or coercivity at room temperature, indicating that they possess a superparamagnetic character. The saturation magnetization (M_S) values of Fe_3O_4, Fe_3O_4@Initiator, and Fe_3O_4@PAAPBA MNPs were 45.7, 41.7 and 27.4 emu g^{-1}, respectively (Figure 5). Although the values of Fe_3O_4@PAAPBA was a little lower than that of Fe_3O_4, the relatively large M_S value was sufficient to fulfill the swift and efficient separation from the solution in only 1 min in the presence of an external magnet (Fig. 5 inset).

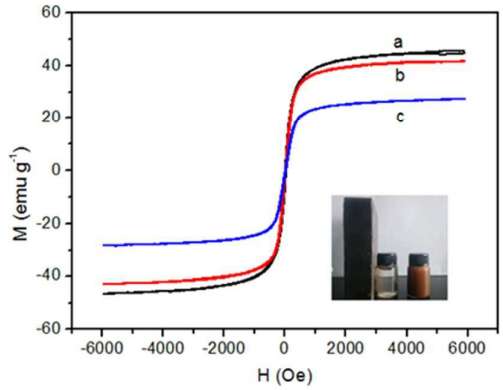

Figure 5 Vibrating sample magnetometry curves of Fe_3O_4 (a), Fe_3O_4@Initiator (b), and Fe_3O_4@PAAPBA (c) MNPs.

The thermogravimetric analysis (TGA) curves of Fe_3O_4, Fe_3O_4@Initiator, and Fe_3O_4@PAAPBA MNPs are shown in Figure 6. It can be seen that about 15% weight loss is observed on the curve of citrate stabilized Fe_3O_4 MNPs (curve a) corresponding to the evaporation of the adsorbed solvent and the decomposition of citrate. As for the Fe_3O_4@Initiator MNPs (curve b), an additional 4% weight loss is due to the decomposition of APTES and the grafted initiator. As shown in Figure 6b and c, there existed a 13% weight difference between Fe_3O_4@Initiator and Fe_3O_4@PAAPBA MNPs related to the PAAPBA layer, which means that the polymeric layer content was about 13 wt%. The results of TGA is consistent with the TEM images of the Fe_3O_4@Initiator, and Fe_3O_4@PAAPBA MNPs.

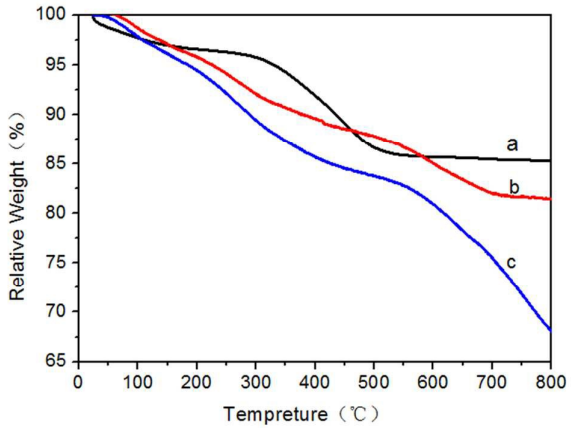

Figure 6 TGA curves of Fe_3O_4 (a), Fe_3O_4@Initiator (b), and Fe_3O_4@PAAPBA (c) MNPs.

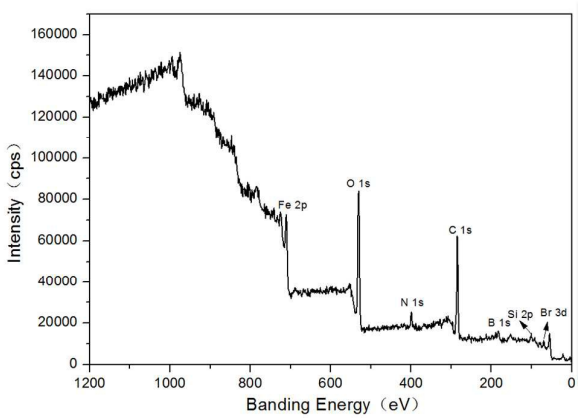

Figure 7 X-ray photoelectron survey spectrum of Fe_3O_4 (a), Fe_3O_4@Initiator (b), and Fe_3O_4@PAAPBA (c) MNPs.

The X-ray photoelectron survey spectrum of the boronic acid ligand-functionalized Fe_3O_4@PAAPBA MNPs is shown in Figure 7. The XPS spectrum shows a C 1s peak around 284 eV, O 1s peak at 531 eV, Fe 2p peak at 710 eV, N 1s at 399 eV, Br 3d peak at 73eV, Si 2p at 102 eV and B1s peak at 184 eV. The elements C, O, B, Fe, N, Br, Si appeared on the surface of the Fe_3O_4@PAAPBA MNPs demonstrated that each step of chemical reaction leading to the preparation of Fe_3O_4@PAAPBA MNPs was successful.

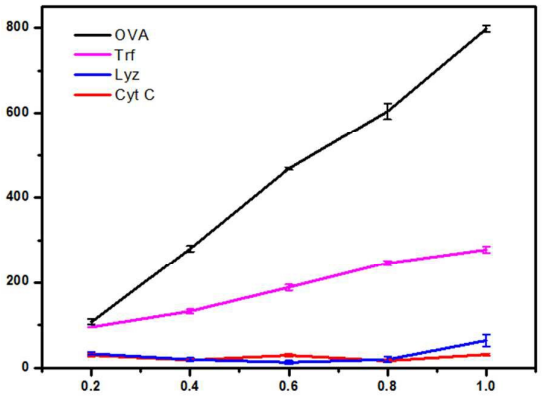

Figure 8 Adsorption of four proteins (OVA, Trf, Lyz and CytC) on Fe_3O_4@PAAPBA MNPs.

3.2 The enrichment and separation of glycoproteins

In order to investigate the binding properties and selectivity of the Fe_3O_4@PAAPBA MNPs towards glycoproteins, two types of glycoproteins OVA, Trf and two types of nonglycoproteins Lyz, Cyt C were chosen as analytes. Generally, boronic acid covalently form cyclic esters with the *cis*-diol moiety in an alkaline solution, and the

reversible boronate esters can dissociate when switching the medium acidic, allowing the target molecules to be released. Specifically, Fe_3O_4@AAPBA MNPs were incubated with protein solutions of various concentrations (0.2–1.0 mg mL^{-1}) in 0.02 M phosphate buffer solution (PBS) containing 0.5 M NaCl (pH 9.0). The purpose of adding NaCl is to sufficiently suppress nonspecific electrostatic interaction between basic proteins Lyz (pI 10.7) and Cyt C (pI 9.8) with boronic acid ligands. The adsorption isotherms of the Fe_3O_4@PAAPBA MNPs towards four proteins at pH 9.0 are shown in Figure 8. It can be seen from the Figure 8, the Fe_3O_4@PAAPBA MNPs showed remarkable specific binding to glycoproteins OVA and Trf than to nonglycoproteins Lyz and Cyt C. The binding capacity of Fe_3O_4@PAAPBA MNPs towards 1.0 mg mL^{-1} glycoproteins OVA and Trf is 798.1 and 278.1 mg g^{-1} respectively. In contrast, the adsorption of nonglycoproteins CytC and Lyz was much less than that of the glycoproteins on the MNPs, the adsorption capacity is 53.7 mg g^{-1} for Lyz, 30.8 mg g^{-1} for Cyt C. The binding capacity of Fe_3O_4@PAAPBA MNPs towards glycoproteins depends on the amount of boronic acid on the surface. We estimated the amount of boronate by the content of the element Br on the surfaces of the Fe_3O_4@Initiator based on the assumption that the Br atoms were displaced by boronate ligands. The amount of Br atoms, which was measured by ion chromatography and the relative masses of Br were 8% (wt%). The high content of the initiator made more boronic acid ligands to graft on the surface of microspheres. The results of this adsorption experiment also demonstrated the efficiency and potential of using ATRP method to synthesize boronate affinity materials.

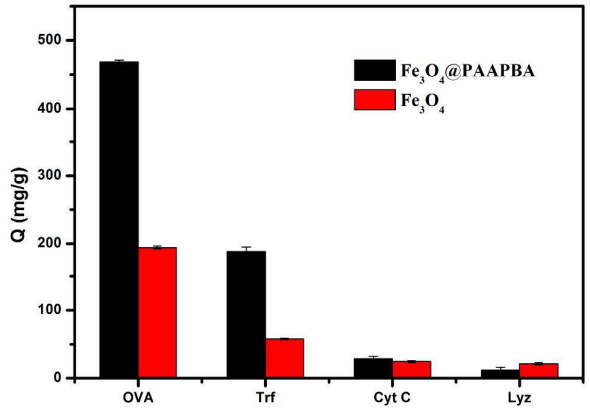

Figure 9 Adsorption of four proteins (OVA, Trf, Lyz and Cyt C) in the concentrations of 0.6 mg mL^{-1} on Fe_3O_4 and Fe_3O_4@PAAPBA MNPs.

To further prove the boronate affinity interaction, we used Fe_3O_4 MNPs and Fe_3O_4@PAAPBA MNPs respectively to examine the nonspecific and specific adsorption of 0.6 mg mL^{-1} for four proteins. As shown in Figure 9, in comparison with Fe_3O_4@PAAPBA MNPs, the unmodified Fe_3O_4 MNPs displayed little binding capacity to the two glycoproteins OVA and Trf. But as to the two nonglycoproteins, the adsorption capacity showed no significant differences between Fe_3O_4 and Fe_3O_4@PAAPBA MNPs. It indicated that boronate affinity interactions were dominant to the adsorption of glycoproteins. The nonspecific binding might be due to the large number of hydroxyl on the surface of the unmodified Fe_3O_4 MNPs.

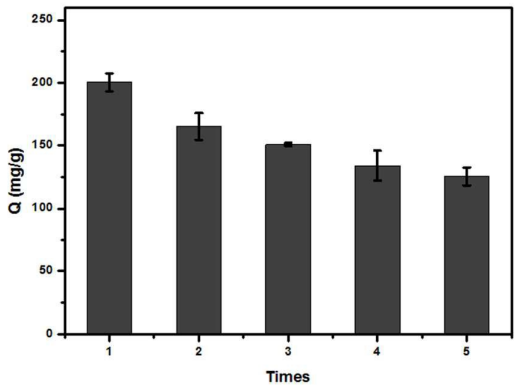

Figure 10 Reusabilityof Fe_3O_4@PAAPBA MNPs through the adsorption–regeneration cycle.

Reusability is another important property in the application of adsorbents. To examine the reusability of Fe_3O_4@PAAPBA MNPs, the adsorption–desorption cycle was repeated five times. The Fe_3O_4@PAAPBA MNPs were incubated with 0.6 mg ml^{-1} Trf in 20 mM phosphate buffer solution containing 0.5 M NaCl (pH 9.0) . After being separated with the magnetic field, the adsorbed Trf could be eluted by using acidic eluent (pH 4.0). The results show that after five times of the adsorption–desorption cycle, the Fe_3O_4@PAAPBA MNPs could still maintain a considerable adsorption capacity (Figure 10).

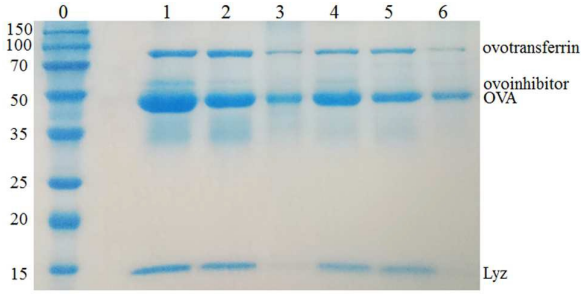

Figure 11 SDS-PAGE analysis of egg white samples with Fe_3O_4@PAAPBA MNPs: lane 0, protein marker; lane 1, 200-fold dilution of egg white before treatment; lane 2, 200-fold dilution of egg white after adsorption by Fe_3O_4@PAAPBA MNPs; lane 3, eluent of proteins captured from 200-fold dilution of egg white; lane 4, 400-fold dilution of egg white before treatment; lane 5, 400-fold dilution of egg white after adsorption by Fe_3O_4@PAAPBA MNPs; lane 6, eluent of proteins captured from 400-fold dilution of egg white.

To demonstrate the feasibility of practical application of Fe_3O_4@PAAPBA MNPs, we used them to enrich glycoproteins directly from real egg white samples. The egg white sample was diluted 200-fold and 400-fold by 20 mM pH 9.0 PBS containing 0.5 M NaCl. Then, the captured proteins were eluted by acidic eluent (pH 4.0). Finally, dodecyl sulphate polyacrylamide gel electrophoresis (SDS-PAGE) was used to visualize protein samples.

The results of SDS-PAGE analysis are shown in Figure 11, it can be seen that the bands of ovotransferrin (76.7 kDa), ovoinhibitor (49 kDa), OVA (46 kDa) and Lyz (14.4 kDa) were observed in the 200-fold and 400-fold dilutions of egg white without treatment by Fe_3O_4@PAAPBA MNPs (lane 1 and 4), the former three of which are glycoproteins. It is known that OVA exists about 65 percent in the egg white sample.[37] It is obvious that the bands of glycoproteins ovotransferrin, ovoinhibitor and OVA faded after they were adsorbed by Fe_3O_4@PAAPBA MNPs, while the band of nonglycoprotein Lyz (14.4 kDa) remained the same (lane 2 and lane 5). After the adsorbed proteins on the Fe_3O_4@pAAPBA MNPs were eluted, the bands of the adsorbed glycoproteins reappeared in the eluted solution and no appreciable amount of Lyz could be detected (lane 2 and lane 5). The results confirmed that the Fe_3O_4@PAAPBA MNPs have the ability to selectively capture glycoproteins from complex biological samples.

4. Conclusions

In this work, a facile and efficient approach for synthesize boronate affinity ligand-functionalized magnetic nanoparticles by surface-initiated atom transfer radical polymerization has been developed. The resulting Fe_3O_4@PAAPBA MNPs have uniform and spherical morphology with the average diameters of ~300 nm, which showed superior magnetic responsibility, the superparamagnetic core in the microspheres enables them to be isolated by an external magnetic field. The Fe_3O_4@PAAPBA MNPs exhibit excellent specificity and high binding capacity towards glycoproteins, and also have a good reusability. Furthermore, a practical application of Fe_3O_4@PAAPBA MNPs was successfully demonstrated in enrichment and isolation of glycoproteins from real egg white samples. Therefore, the Fe_3O_4@PAAPBA MNPs were expected to be promising affinity materials in the glycoproteomic analysis.

Acknowledgements

The authors are grateful to the National Basic Research Program of China (No. 2012CB910601), the National Natural Science Foundation of China (No. 21275080, 21475067) and the National Natural Science Foundation of Tianjin (No. 15JCYBJC20600).

Notes and references

1 G. A. Rabinovich and M. A. Toscano, *Nat. Rev. Immunol*, 2009, **9**, 338.
2 G. W. Hart and R. J. Copeland, *Cell*, 2010, **143**, 672.
3 J. Hirabayashi, T. Hashidate and K. Kasai, *J. Biomol. Tech.,* 2002, **13**, 205.
4 C. A. Reis, H. Osorio, L. Silva, C. Gomes and L. David, *J. Clin. Pathol.*, 2010, **63**, 322.
5 H. Narimatsu, H. Sawaki, A. Kuno, H. Kaji, H. Ito and Y. Ikehara, *FEBS J*, 2010, **277**, 95.
6 Y. Zhang, M. Kuang, L. Zhang, P. Yang and H. Lu, *Anal. Chem.*, 2013, ***85,*** 5535.
7 Z. Xiong, H. Qin, H. Wan, G. Huang, Z. Zhang, J. Dong, L. Zhang, W. Zhang and H. Zou, *Chem. Commun.*, 2013, **49**, 9284.
8 M. Caragata, A. K. Shah, B. L. Schulz, M. M. Hill and C. Punyadeera, *Anal. Biochem.,*2016, **497**, 76.
9 Y. Li, P. Shah, A. M. De Marzo, J. E. Van Eyk, Q. Q. Li, D. W. Chan and H. Zhang, *Anal. Chem.,* 2015, **87**, 4683.
10 Y. Zhang, M. Yu, C. Zhang, W. Ma, Y. Zhang, C. Wang, H. Lu, *Anal. Chem.*, 2014, **86**, 7920.
11 J. Liu, K. Yang, Y. Qu, S. Li, Q. Wu, Z. Liang, L. Zhang, and Y. Zhang, *Chem. Commun.*, 2015, **51**, 3896.
12 W. Cong, A. Zhou, Z. Liu, J. Shen, X. Zou, W. Ye, Z. Zhu, X. Zhu, J. Lin and L. Jin, *Anal. Chem.,* 2015, **87**, 1462.
13 H. Wan, J. Huang, Z. Liu, J. Li, W. Zhang, H. Zou, *Chem. Commun.*, 2015, **51**, 9391.
14 C. F. Bi, Y. R. Zhao, L. J. Shen, K. Zhang, X. W. He, L. X. Chen, Y. K. Zhang, *ACS Appl. Mater. Interfaces*, 2015, **7**, 24670.
15 C. F. Bi, R. D. Jiang, X. W. He, L. X. Chen, Y. K. Zhang. *RSC Advances*, 2015, **5**, 59408.
16 Y. Qu, J. Liu, K. Yang, Z. Liang, L. Zhang and Y. Zhang, *Chem. Eur. J.*, 2012, **18**, 9056.
17 Y. Guan, Y. J. Zhang, *Chem. Soc. Rev.*, 2013, **42**, 8106.
18 Z. Lin, J. Pang, H. Yang, Z. Cai, L. Zhang and G. Chen, *Chem. Commun.*, 2011, **47**, 9675.
19 F. Yang, Z. Lin, X. He, L. Chen and Y. Zhang, *J. Chromatogr. A.*, 2011, **1218**, 9194.
20 F. Yang, J. Mao, X. W. He, L. X. Chen and Y. K. Zhang, *Anal. Bioanal. Chem.,* 2013, **405**, 5321.
21 L. Liu, Y. Zhang, L. Zhang, G. Yan, J. Yao, P. Yang and H. Lu, *Anal. Chim. Acta*, 2012, **753**, 64.
22 R. Ma, J. Hu, Z. Cai and H. Ju, *Nanoscale*, 2014, **6**, 3150.
23 Z. A. Lin, J. N. Zheng, F. Lin, L. Zhang, Z. Cai and G. N. Chen, *J. Mater. Chem.*, 2011, **21**, 518.
24 X. Zhang, X. He, L. Chen and Y. Zhang, *J. Mater. Chem.*, 2012, **22**, 16520.
25 X. Zhang, X. He, L. Chen and Y. Zhang, *J. Mater. Chem. B.*, 2014, **2**, 3254.
26 S. Zhang, X. He, L. Chen and Y. Zhang, *New J. Chem.*, 2014, **38**, 4212.
27 J. Liu, Y. Qu, K. Yang, Q. Wu, Y. Shan, L. Zhang, Z. Liang and Y. Zhang, *ACS Appl. Mater. Interfaces*, 2014, **6**, 2059.
28 X. H. Zhang, J. W. Wang, X. W. He, L. X. Chen, Y. K. Zhang, *ACS Appl. Mater. Interfaces,* 2015, **7**, 24576.
29 K. Matyjaszewski, T. E. Pattern and J. Xia, *J. Am. Chem. Soc.* ,1997, **119** , 674.
30 K. Matyjaszewski and N. V. Tsarevsky, *Nat. Chem*, 2009, **1**, 276.
31 K. Matyjaszewski, J. H. Xia, *Chem. Rev.,* 2001, **101**, 2921.
32 J. Pyun, T. Kowalewski and K. Matyjaszewski, *Macromol. Rapid Commun.,* 2003, **24**, 1043.
33 C. H. Lu, Y. Wang, Y. Li, H.-H. Yang, X. Chen and X.R. Wang, *J. Mater. Chem.*, 2009, **19**, 1077.
34 X. D. Mao, H. Y. Sun, X. W. He, L. X. Chen, Y. K. Zhang, *Anal. Methods*, 2015, **7**, 4707.
35 S. Xuan, Y.X. J. Wang, J. C. Yu and K. C. F. Leung, *Chem. Mater.,* 2009, **21**, 5079.
36 R. X. Gao, X. Kong, X. Wang, X. W. He, L. X. Chen, Y. K. Zhang, *J. Mater. Chem.*, 2011, **21**, 17863.
37 J. A. Huntington and P. E. Stein, *J. Chromatogr. B*, 2001, **756**, 189.

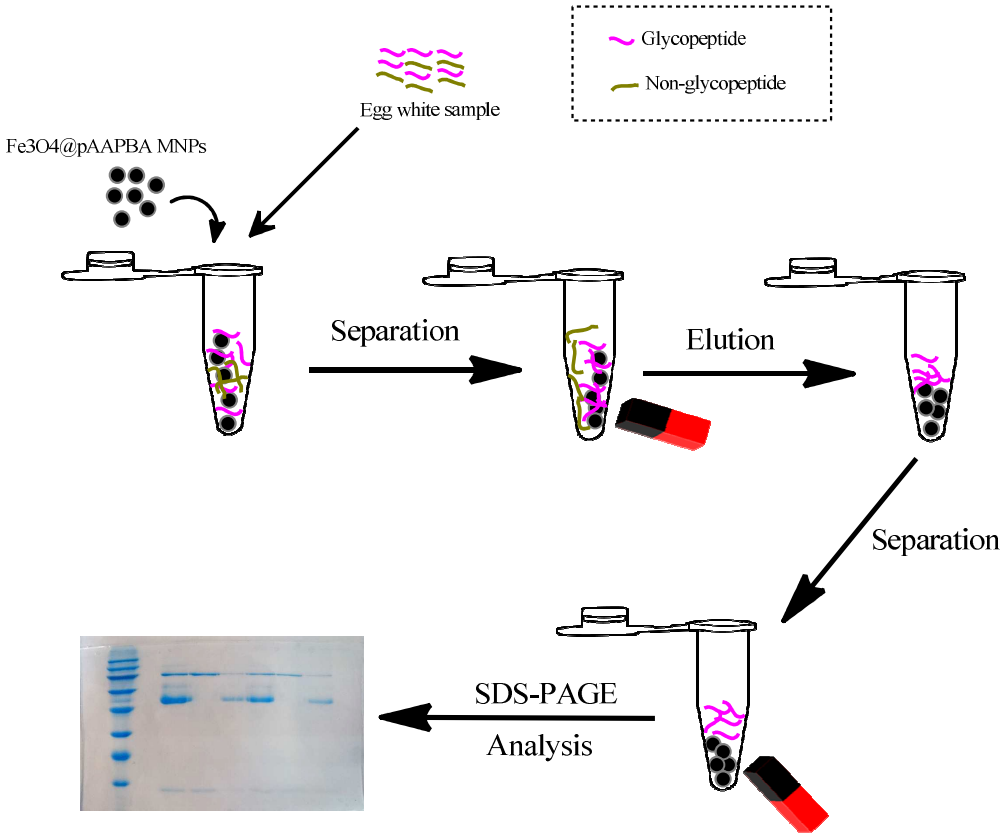

A facile and efficient approach to synthesize boronate affinity ligand-functionalized magnetic nanoparticles for specific enrichment of glycoproteins *via* surface-initiated atom transfer radical polymerization (SI-ATRP) has been developed.